Proceedings of *RAGtime ?/?, ?–?/?–? September, ????/????, Opava, Czech Republic*
S. Hledík and Z. Stuchlík, editors, Silesian University in Opava, ????, pp. 1–14

arXiv:1411.4690v1 [astro-ph.HE] 17 Nov 2014

Eigenmodes of trapped horizontal oscillations in accretion disks

S. Khanna[1], Z. Strzelecka[2], B. Mishra[3], W. Kluźniak[3]

[1]Leiden Observatory, Leiden University, PO Box 9513,
2300 RA Leiden, The Netherlands
[2]Imperial College London, Department of Physics, Blackett Laboratory,
Prince Consort Road, London SW7 2BB, United Kingdom
[3]Nicolaus Copernicus Astronomical Center, Bartycka 18, 00-716 Warsaw, Poland

ABSTRACT

We present eigenfrequencies and eigenfunctions of trapped acoustic-inertial oscillations of thin accretion disks for a Schwarzschild black hole and a rapidly rotating Newtonian star (a Maclaurin spheroid). The results are derived in the formalism of Nowak and Wagoner (1991) with the assumption that the oscillatory motion is parallel to the midplane of the disk. The first four radial modes for each of five azimuthal modes ($m = 0$ through $m = 4$) are presented. The frequencies and wavefunctions of the lowest modes may be accurately approximated by Airy's function.

Keywords: Relativistic stars: black holes, structure stability and oscillations, relativity and gravitation, accretion disks, hydrodynamics

1 TRAPPED MODES

Kato and Fukue (1980) showed that acoustic-inertial modes may be trapped in the inner parts of an accretion disk. This occurs when the (radial) epicyclic frequency κ has a maximum, as is the case in the Schwarzschild metric of general relativity (GR) considered by the authors. Okazaki et al. (1987); Kato (1989) and Nowak and Wagoner (1991, 1992) consider a model of a black hole accretion disk in hydrostatic equilibrium, and derive a dispersion relation for modes with $n = 0, 1, 2, 3..$ nodes along the z-axis (the symmetry axis of the disk). The trapping occurs for oscillation frequencies below the maximum of the epicyclic frequency $\omega < \kappa_{\rm max}$. Here $\omega(r) = m\Omega(r) + \sigma$ is the frequency in the frame co-rotating with the fluid (at angular frequency Ω), m is the azimuthal mode number, σ is the eigenfrequency of the mode, and $\kappa^2 = (2\Omega/r)\mathrm{d}(r^2\Omega)/\mathrm{d}r$. The $n = 0$ modes will be trapped between the inner edge of the disk, close to the ISCO at $\kappa(r_{\rm ms}) = 0$, and the lowest radius r satisfying $\omega(r) = \kappa(r)$, while for $n = 1$ trapping occurs close to the maximum of κ, between those two radii at which $\omega = \kappa$. Further discussion can be found in the

NO-ISBN-SET-X © ???? – SU in Opava. All rights reserved.

textbook by Kato et al. (1998). In this contribution we only consider the $n = 0$ trapped modes.

Currently, the main interest in disk oscillations is related to the observed frequencies in the X-ray flux from black hole and neutron star systems (for a review see van der Klis M., 2000). For black hole disks the modes thought to be offering the most promising explanation (Wagoner et al., 2001) of the highest observed frequencies are the g-modes and c-modes, investigated in full GR by Perez et al. (1997); Silbergleit et al. (2001), although a different explanation seems to be required for the observed 3:2 ratio of the highest frequencies in the microquasars (Abramowicz and Kluźniak, 2001; Kluźniak et al., 2004; Török et al., 2005). Thus, the modes investigated here are not prime candidates for a theoretical counterpart to the observed high frequency QPOs (quasi-periodic oscillations) in black hole systems. However, similar phenomena are observed in white dwarf systems (Woudt and Warner, 2002), and while their harmonic content may be explained by a resonance (Kluźniak et al., 2005), the origin of the observed frequencies remains obscure. For this reason we would like to discuss disk oscillations in a framework valid equally in a GR and non-GR context.

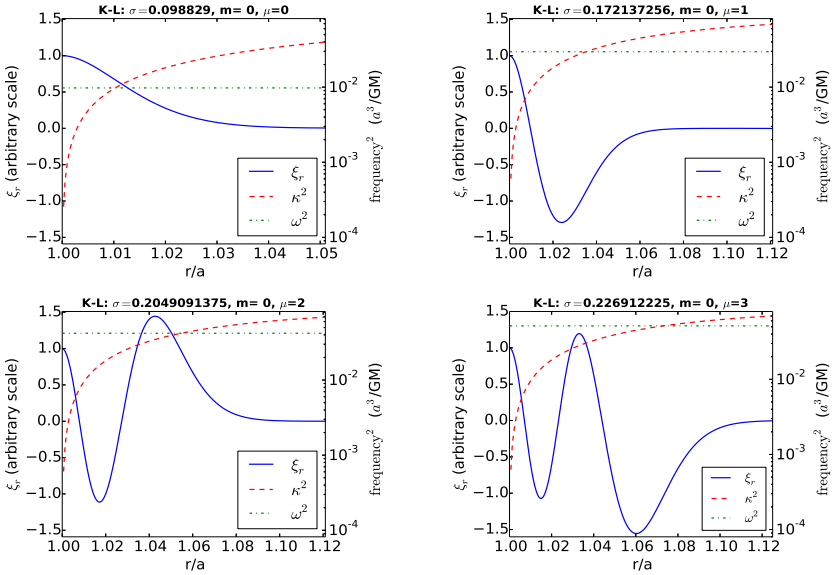

Figure 1. The fundamental and the first three radial overtones for $m = 0$ trapped horizontal oscillations of a thin ($H/a = 10^{-3}$) accretion disk for the potential of Eq. (4). Plotted are the wavefunction: solid (blue) line (arbitrary normalization, left scale); $\omega^2(r)/\Omega^2(r_{\rm ms})$: dashed-dotted (green) line and $\kappa^2(r)/\Omega^2(r_{\rm ms})$: dashed (red) line (logarithmic scale, right).

2 EQUATION OF MOTION AND THE BOUNDARY CONDITION

We will be closely following the approach of Nowak and Wagoner (1991) who describe perturbations with a Lagrangian displacement vector in cylindrical coordinates $(\xi^r_*, \xi^\phi_*, \xi^z_*) = (\xi^r, \xi^\phi, \xi^z)\exp[i(m\phi + \sigma t)]$ in the formalism of Friedman and Schutz (1978), and show that in the WKB approximation the azimuthal component of the equation of perturbed motion for thin disks reduces to $\xi^\phi = 2i\big(\Omega/\omega\big)\xi^r$. In this contribution we assume horizontal motion, implying that $\xi^z_* \equiv 0$ and $\partial\xi^r_*/\partial z \equiv 0$. In terms of $\Psi(r) \equiv \sqrt{\gamma Pr}\,\xi^r(r)$ the remaining component of the equation of motion then gives

$$\frac{\mathrm{d}^2\Psi}{\mathrm{d}r^2} + \frac{(\omega^2 - \kappa^2)}{c_\mathrm{s}^2}\Psi = 0, \tag{1}$$

where $c_\mathrm{s}^2 = \gamma P/\rho$ is the speed of sound squared; the boundary condition is that the Lagrangian perturbation of pressure vanishes at the unperturbed boundary, $\Delta P \equiv \gamma P \nabla\xi_* = 0$, which reduces to

$$\frac{1}{r}\frac{\partial}{\partial r}(r\xi^r_*) + \frac{1}{r}\frac{\partial}{\partial\phi}(\xi^\phi_*) = 0$$

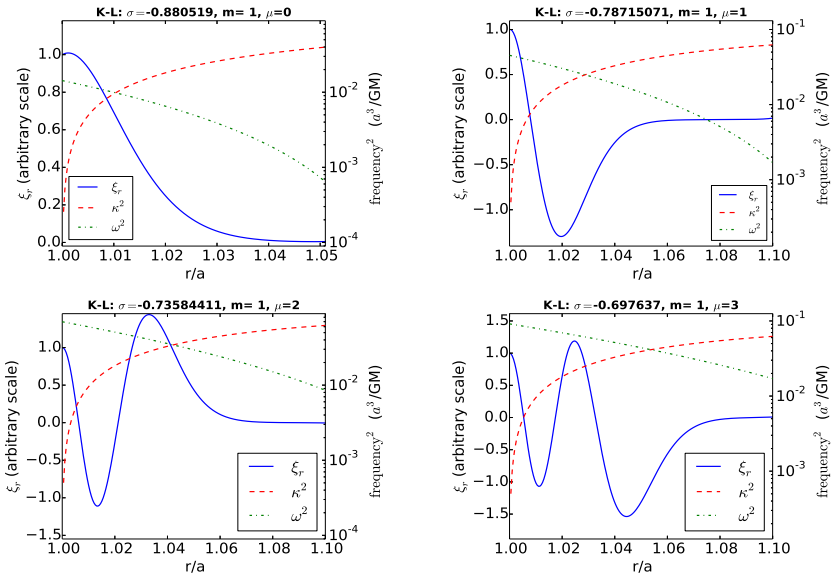

Figure 2. Same as Fig. 1, but for $m = 1$.

assuming that $P \neq 0$ (Nowak and Wagoner, 1991). Neglecting derivatives of P this gives our final boundary condition at the inner edge, at $r = a$, which we will take to be at the marginally stable orbit (ISCO) at $a = r_{\rm ms}$,

$$\frac{\mathrm{d}\Psi}{\mathrm{d}r} = -\frac{\Psi}{2r}\big(1 - 4m\Omega/\omega\big).$$

In dimensionless form, with $r = a(1+x)$, $\tilde{\omega}(x) = \omega(r)/\Omega(a)$, $\tilde{\kappa}(x) = \kappa(r)/\Omega(a)$, $\tilde{\sigma} = \sigma/\Omega(a)$, and $c_{\rm s} = H\Omega(a)$, the perturbation (wave) equation takes the form

$$\frac{\mathrm{d}^2\Psi}{\mathrm{d}x^2} + \left(\frac{a}{H}\right)^2 \left(\tilde{\omega}^2 - \tilde{\kappa}^2\right)\Psi = 0, \tag{2}$$

with the boundary condition at $x = 0$

$$\frac{\mathrm{d}\Psi}{\mathrm{d}x} = -\frac{\Psi}{2}\big(1 - 4m/\tilde{\omega}\big). \tag{3}$$

In the last equation $\tilde{\omega} = \tilde{\sigma} + m$. Recall that in general $\tilde{\omega}(x) = \tilde{\sigma} + m\Omega(r)/\Omega(a)$.

In this contribution we are providing an atlas of eigenfrequencies and eigenfunctions for the fundamentals and the first three radial overtones of horizontal disk oscillations (labeled with the number of radial nodes, $\mu = 0, 1, 2, 3$) for $m = 0, 1, 2, 3, 4$.

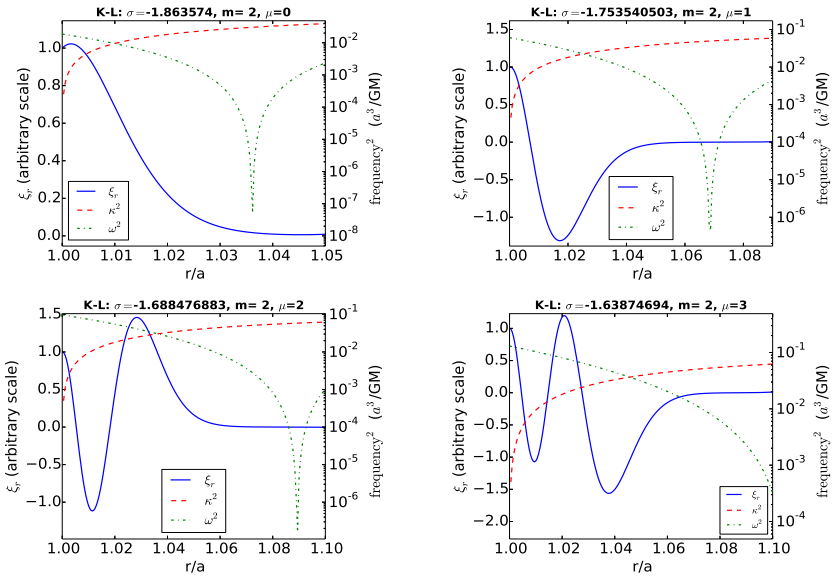

Figure 3. Same as Fig. 1, but for $m = 2$.

3 MODELS OF A SCHWARZSCHILD BLACK HOLE

Bohdan Paczyński showed that it is possible to capture essential qualitative features of motion in the Schwarzschild metric in a Newtonian model with a simple pseudo-potential $\Phi(r) = -GM/(r - 2r_g)$ (Paczyński and Wiita, 1980), with $r_g = GM/c^2$. Nowak and Wagoner (1991) found the eigenfrequencies and eigenfunctions of Eq. (1) for the fundamental oscillations with $m = 0$, and $m = 2$, using values of $\kappa^2(r)$ following from their own pseudo-potential $\Phi(r) = -(GM/r)[1 - 6r_g/r + 12(r_g/r)^2]$.

Here, we model the Schwarzschild metric with a Newtonian pseudo-potential designed expressly to reproduce the Schwarzschild ratio of $\kappa^2(r)/\Omega^2(r) = 1 - 6r_g/r$:

$$\Phi_{\rm KL}(r) = -(c^2/6)\exp(6r_g/r - 1). \tag{4}$$

As we are only interested in the inner parts of an accretion disk, we have dropped an additive constant. We have also renormalized the original form of the potential (Kluźniak and Lee, 2002) by a factor of $1/e$ to guarantee the correct value of $\Omega(r_{\rm ms})$. The angular frequency of orbital motion follows from $\Omega^2(r) = r^{-1}\partial\Phi_{\rm KL}/\partial r$ and, as for the other two potentials, the marginally stable orbit comes out to be at $r_{\rm ms} = 6GM/c^2$. We have numerically solved the eigenvalue problem given by Eqs. (2), (3), for $H/a = 10^{-3}$. The equations being linear in Ψ, we normalize the wavefunction to unity at the inner edge of the disk: $\Psi(r_{\rm ms}) = 1$. Fig. 1 presents the eigenfrequencies

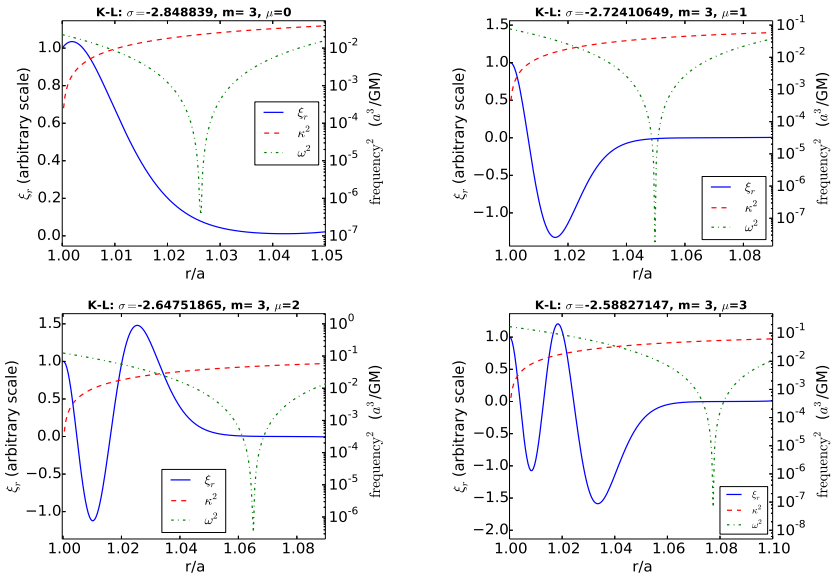

Figure 4. Same as Fig. 1, but for $m = 3$.

σ and the eigenfunctions $\Psi(r)$ for $m = 0$ and $\mu = 0, 1, 2, 3$, while Figs. 2, 3, 4, 5 present the same quantities, as well as $\tilde{\omega}^2$, for $m = 1, 2, 3, 4$, respectively.

4 ESSENTIALS OF ACOUSTIC-INERTIAL OSCILLATIONS

4.1 Wave equation

Dust orbiting an axially symmetric gravitating body in its equatorial plane ($z = 0$) would settle in stable circular orbits. The orbit of each dust particle being stable, it corresponds to "rest" (we are only concerned with radial motion in this section) at a fixed radial distance from the center of the body in the minimum of the effective potential, $V(r, z) = \Phi(r, z) + l^2/(2r^2)$, $l \equiv r^2\Omega(r)$ being the conserved angular momentum of a given particle, and Φ the gravitational potential of the body, both per unit mass. Consider small radial perturbations δr of motion of a dust disk (such as the rings of Saturn). Neglecting particle collisions, the perturbed dust would be executing radial harmonic (epicyclic) motion with respect of the stable orbits. The square of the frequency of this radial motion, $\kappa^2 = \partial^2 V/\partial^2 r$ corresponds to the strength of the restoring force per unit mass: $-\kappa^2\psi_*$ (if we denote the radial

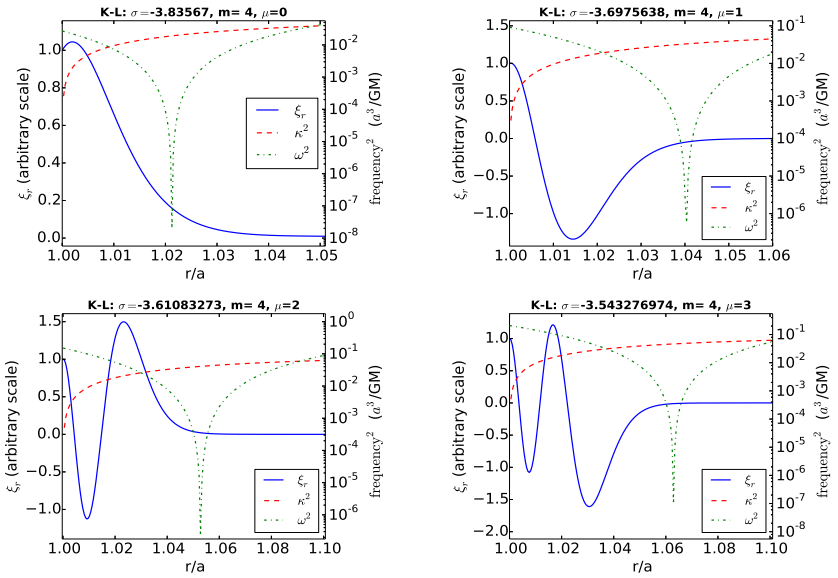

Figure 5. Same as Fig. 1, but for $m = 4$.

displacement $\delta r = \psi_*$). If the dust disk is replaced by a fluid, there will be an additional restoring force corresponding to pressure perturbations.

It is well known that sound waves in a homogeneous medium can be described by a harmonic function both in space and in time, with a constant and uniform amplitude if attenuation is neglected. Thus, the acoustic displacement of the fluid satisfies both a wave equation

$$\frac{\partial^2 \psi_*}{\partial y^2} + k_{\rm s}^2 \psi_* = 0, \tag{5}$$

and an oscillator equation

$$\frac{\partial^2 \psi_*}{\partial t^2} + \omega_{\rm s}^2 \psi_* = 0, \tag{6}$$

corresponding to a restoring force $-\omega_{\rm s}^2 \psi_*$. The frequency of the sound wave is related to the wave vector through the linear dispersion relation

$$k_{\rm s}^2 = \omega_{\rm s}^2 / c_{\rm s}^2. \tag{7}$$

Clearly, taking into account in the oscillator equation both the "inertial" (epicyclic) and the acoustic restoring forces, and neglecting for the moment the difference be-

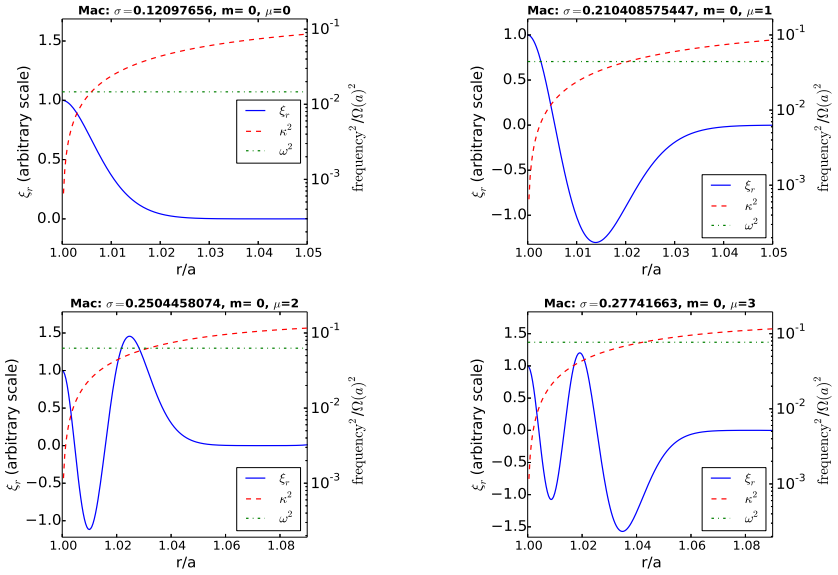

Figure 6. Same as Fig. 1, but for the potential of a Maclaurin spheroid with ellipticity $e = 0.834583178$.

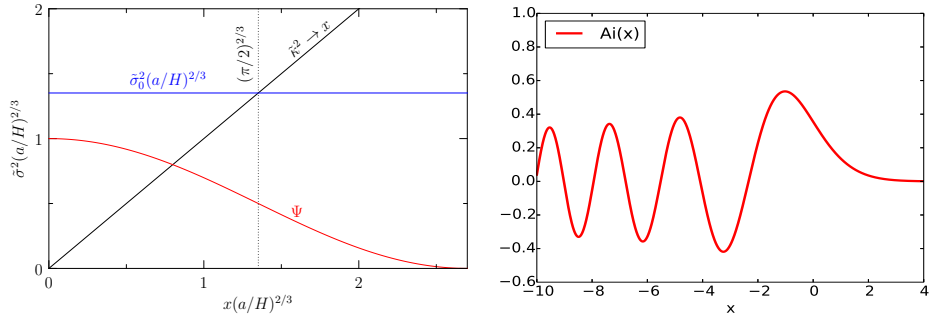

Figure 7. *Left Panel:* A simple approximation to the eigenfrequency $\tilde{\sigma}_0$ of the axisymmetric fundamental mode ($m = 0, \mu = 0$): a quarter wavelength fits in the inner region of the disk ($\tilde{\sigma}_0^2 \geq \tilde{\kappa}^2$) before the wave becomes evanescent. The vertical dotted line indicates the value of x at which $\tilde{\sigma}_0^2$ and x must intersect for this condition to be met: $\tilde{\sigma}_0^2 = \tilde{\kappa}^2(x_0) \approx x_0$, with $x_0 = (\pi/2)^{2/3} \cdot (H/a)^{2/3}$. The diagonal solid (black) line corresponds to the linear approximation $\tilde{\kappa}^2(x) = x + \mathcal{O}(x^2)$, which is valid for the potential of Eq. (4). See Eq. (9) and Section 4.2 for details
Right Panel: A better approximation is obtained from the location of the extrema of Airy's function $\mathrm{Ai}(X)$. Note that the shape of $\mathrm{Ai}(X)$ closely resembles the shape of the numerically found $\Psi(x)$.

tween the cylindrical co-ordinate r and the Cartesian co-ordinate y, the acoustic-inertial displacement of the fluid can be described by a displacement $\psi_*(y,t) = \psi(y)\exp(i\omega t)$, with $\omega^2 = \kappa^2 + \omega_\mathrm{s}^2$ (or, in the form written down by Binney and Tremaine, 1987, $\omega^2 = \kappa^2 + k_\mathrm{s}^2 c_\mathrm{s}^2$). Substituting this new dispersion relation into Eq. (7), we see that Eq. (5) takes the form

$$\frac{\mathrm{d}^2\psi}{\mathrm{d}y^2} + \frac{\omega^2 - \kappa^2}{c_\mathrm{s}^2}\psi = 0. \tag{8}$$

Remarkably, this is the same equation that was rigorously derived by Nowak and Wagoner (1991), i.e., Eq. (1). In the remainder of this paper we will be discussing numerical solutions of its dimensionless version, Eq. (2), subject to the boundary condition Eq. (3), for a thin disk ($H/a = 0.001$) in two different models of the gravitating body, i.e., for two different epicyclic frequencies $\kappa(r)$.

4.2 Estimates of the eigenfrequencies

It is possible to understand the values of the eigenfrequencies σ and the shape of the wavefunctions in a simple model of Eq. (2). For axially symmetric modes, $m = 0$ and hence $\omega = \sigma$. The wave equation has oscillatory solutions for $\omega^2 > \kappa^2$, while the wave is evanescent for $\omega^2 < \kappa^2$. Thus the mode is trapped between $a = r_\mathrm{ms}$ (i.e., $x = 0$) and $r = r_0$ such that $\sigma^2 = \kappa^2(r_0)$ (Fig. 7).

As $\sigma^2 << \kappa^2_{\rm max}$ for the fundamental mode and $\kappa^2(r_{\rm ms}) = 0$ we can model κ^2 with a linear approximation (Nowak and Wagoner, 1991), which for the potential of Eq. (4) has the simple form $\tilde{\kappa}^2 = x$. Thus, the wave becomes evanescent at $r_0/a - 1 = x_0 \approx \tilde{\sigma}^2$. We can take the boundary condition on the wave to correspond to that of a banner flapping in the wind, with a crest at the edge [of the disk ($x = 0$)] and a node close to x_0. Perhaps a quarter wavelength of a sinusoid between $x = 0$ and $x = x_0$ is a fair approximation (Kato and Fukue, 1980).

With the above approximations, we have $ax_0 = \lambda/4$, and $\tilde{\sigma}^2 = x_0$. Now, $k = 2\pi/\lambda \approx \sigma/c_{\rm s}$ so $\lambda/4 \approx \pi c_{\rm s}/(2\sigma) = \pi H\Omega/(2\sigma)$. Recall that $\tilde{\sigma} = \sigma/\Omega(a)$. Finally, we obtain $\tilde{\sigma}^3 = \pi H/(2a)$, yielding

$$\tilde{\sigma} \approx \left(\frac{\pi H}{2a}\right)^{1/3} \approx 1.16 \left(\frac{H}{a}\right)^{1/3}. \qquad (9)$$

For $H/a = 10^{-3}$ this yields $\tilde{\sigma} \approx 0.116$, while the numerically obtained value for the correct functional form of κ^2 is $\tilde{\sigma}_0 \approx 0.0988$. Thus, this crude estimate of the eigenfrequency is off by less than 20%. However, as we will see directly below, we have obtained the correct scaling of the eigenfrequency with the dimensionless thickness of the disk (Kato and Fukue, 1980).

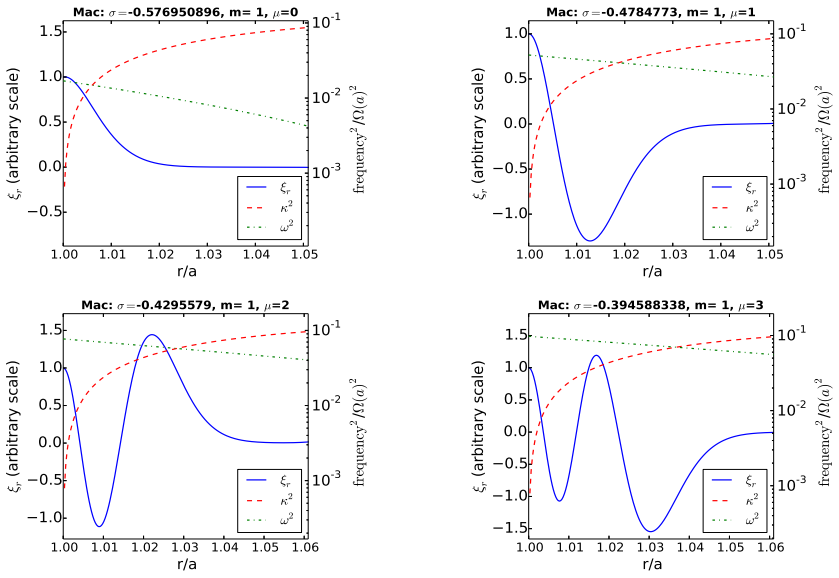

Figure 8. Same as Fig. 6, but for $m = 1$.

A more accurate estimate of the eigenfrequency can be obtained by noting that in the linear approximation to κ^2 (which for the potential of Eq. [4] is simply $\tilde{\kappa}^2 = x$), Eq. (2) corresponds to Airy's equation (Nowak and Wagoner, 1991). Indeed, with the substitution $X = (x - \tilde{\sigma}^2)(a/H)^{2/3}$, Eq. (2) becomes $\mathrm{d}^2\Psi/\mathrm{d}X^2 = X\Psi$, with the Airy function as the solution: $\Psi(X) = \mathrm{Ai}(X)$. In the exact waveforms of Fig. 1, one can recognize the shape of Airy's function, to a good accuracy. The (implicit) eigenvalues $\tilde{\sigma}$ can now be found directly from the boundary condition, Eq. (3), in the form

$$\frac{1}{\Psi}\frac{\mathrm{d}\Psi}{\mathrm{d}X} = \left(\frac{H}{a}\right)^{2/3} \cdot \frac{1}{2}\left(4m/\tilde{\omega} - 1\right).$$

Now, for $H << a$, the boundary condition (at $x = 0$) becomes $\mathrm{d}\log\Psi/\mathrm{d}X << 1$, i.e., it is approximately that X corresponds to one of those X_μ for which $\mathrm{Ai}(X_\mu)$ has an extremum, $\mathrm{dAi}/\mathrm{d}X|_{X_\mu} = 0$. Thus, $\tilde{\sigma}_\mu^2 \approx -(H/a)^{2/3}X_\mu$, $\mu = 0, 1, 2, 3....$ We can compare these approximate eigenfrequencies (Table 1) with the numerically found eigenvalues for the correct form of κ^2. For the fundamental the agreement is quite good, but the accuracy of the Airy approximation gradually degrades as σ_μ approaches the value $\kappa_{\max}$.

Table 1: Exact and approximate eigenvalues of Eqs. (2), (3)

$m = 0,\ H/a = 0.001$	$\mu = 0$	$\mu = 1$	$\mu = 2$	$\mu = 3$
$\tilde{\sigma}_\mu$ for κ^2 of Eq. (4)	0.0988...	0.172...	0.205...	0.227...
Airy approx.: $\sqrt{-0.01X_\mu}$	0.101...	0.180...	0.229...	0.248...
Accuracy of approximation	2%	5%	7%	9%

We thank Mr. Luca Giussani for providing us with the values of Airy's extrema.

5 TRAPPED OSCILLATIONS IN AN ACCRETION DISK AROUND A MACLAURIN SPHEROID

In previous sections, following Nowak and Wagoner (1991) we were discussing the trapped acoustic-inertial oscillations of a pseudo-Newtonian model of an accretion disk around a Schwarzschild black hole. Interestingly, the same trapping phenomenon occurs in strictly Newtonian gravity, for disks orbiting sufficiently oblate bodies. Kluźniak et al. (2001), and Zdunik and Gourgoulhon (2001) pointed out that oblateness of a gravitating body can destabilize orbits close to it, while Amsterdamski et al. (2002) showed that the marginally stable orbit exists in the Newtonian potential of classic Maclaurin spheroids for a sufficiently large ellipticity of the spheroid, i.e., a sufficiently large rotation rate of the spheroid. Kluźniak and Rosińska (2013) give explicit expressions for the angular velocity in circular orbits and for the corresponding epicyclic frequencies as a function of orbital radius and

the ellipticity of the Maclaurin spheroid. Gondek-Rosińska et al. (2014) compare these analytic expressions with exact numerical solutions (in GR) of rapidly rotating quark stars, while Mishra and Vaidya (2014) give accretion disk solutions in the gravitational field of Maclaurin spheroids, which are reminiscent of the Shakura and Sunyaev (1973) black hole accretion disks.

Without further ado, we are presenting the eigenfrequencies and eigenvalues of trapped acoustic-inertial modes for an accretion disk around a Maclaurin spheroid of ellipticity $e = 0.834583178$. We are using the same equation and boundary conditions as before, Eqs. (2), (3), with the functional form of $\kappa^2(r)$ and $\Omega^2(r)$ appropriate for the chosen Maclaurin spheroid. The only other change is that we need to reinterpret H: the condition of hydrostatic equilibrium is $c_{\rm s} = h\Omega_\perp$, with h being the half-thickness of the disk, and $\Omega_\perp$ the vertical epicyclic frequency which we absorb into an effective half-thickness $H = h\Omega_\perp(a)/\Omega(a)$. The results are summarized in Figs. 6, 8, 9, 10, 11 for modes with $m = 0, 1, 2, 3, 4$, respectively. The frequencies are compared in Table (2) with those obtained in the previous sections for the black-hole disk. For both the GR ("KL") and the Newtonian (Maclaurin) $m = 0$ model the ratio of the $\mu = 2$ frequency to the fundamental is very close to 2:1.

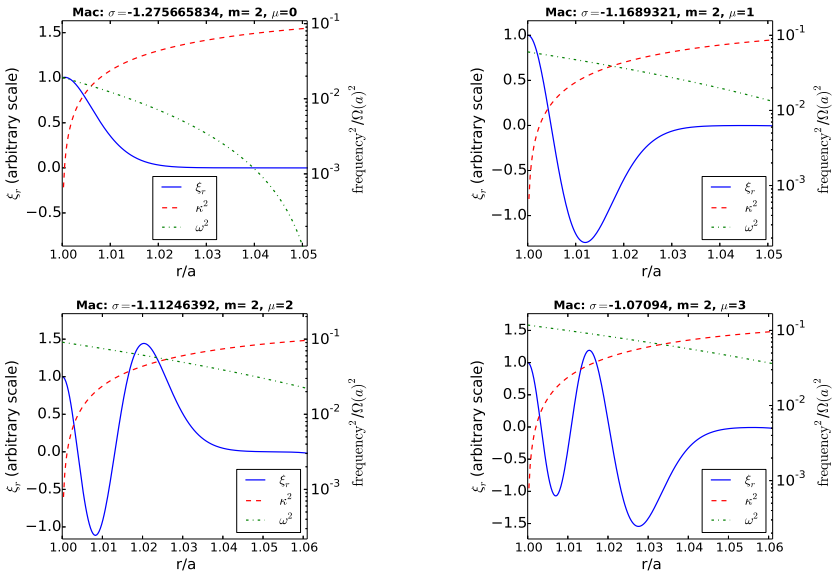

Figure 9. Same as Fig. 6, but for $m = 2$.

Table 2: Eigenvalues of Eqs. (2), (3)

$H/a = 0.001$	$\mu = 0$	$\mu = 1$	$\mu = 2$	$\mu = 3$
KL eq. (4), $m = 0$. $\tilde{\sigma}_\mu =$	0.098829	0.172137	0.204909	0.226912
Maclaurin, $m = 0$. $\tilde{\sigma}_\mu =$	0.120977	0.210409	0.250446	0.277417
KL eq. (4), $m = 1$. $\tilde{\sigma}_\mu =$	-0.880519	-0.787151	-0.735844	-0.697637
Maclaurin, $m = 1$. $\tilde{\sigma}_\mu =$	-0.576951	-0.478477	-0.429558	-0.394588
KL eq. (4), $m = 2$. $\tilde{\sigma}_\mu =$	-1.86357	-1.753541	-1.688477	-1.638747
Maclaurin, $m = 2$. $\tilde{\sigma}_\mu =$	-1.275666	-1.168932	-1.112464	-1.07094
KL eq. (4), $m = 3$. $\tilde{\sigma}_\mu =$	-2.848839	-2.724106	-2.647519	-2.588271
Maclaurin, $m = 3$. $\tilde{\sigma}_\mu =$	-1.974981	-1.860566	-1.797395	-1.750153
KL eq. (4), $m = 4$. $\tilde{\sigma}_\mu =$	-3.83567	-3.697564	-3.610833	-3.543277
Maclaurin, $m = 4$. $\tilde{\sigma}_\mu =$	-2.674776	-2.553138	-2.483865	-2.431476

This work was supported in part by Polish NCN grant 2013/08/A/ST9/00795.

REFERENCES

Abramowicz, M. A. and Kluźniak, W. (2001), A precise determination of black hole spin in GRO J1655-40, *A&A*, **374**, pp. L19–L20.

Amsterdamski, P., Bulik, T., Gondek-Rosińska, D. and Kluźniak, W. (2002), Marginally stable orbits around Maclaurin spheroids and low-mass quark stars, *A&A*, **381**, p. L21.

Binney, J. and Tremaine, S. (1987), Galactic Dynamics, *Princeton University Press*, p. 359.

Friedman, J. L. and Schutz, B. F. (1978), Lagrangian perturbation theory of nonrelativistic fluids, *ApJ*, **221**, p. 937.

Gondek-Rosińska, D., Kluźniak, W., Stergioulas, N. and Wiśniewicz, M. (2014), Epicyclic frequencies for rotating strange quark stars: Importance of stellar oblateness, *Phys. Rev. D*, **89**, p. j4001.

Kato, S. (1989), Low-frequency, one-armed corrugation waves in relativistic accretion disks, *PASJ*, **41**, p. 745.

Kato, S. and Fukue, J. (1980), Trapped radial oscillations of gaseous disks around a black hole, *PASJ*, **32**, p. 377.

Kato, S., Fukue, J. and Mineshige, S. (1998), Black-Hole Accretion Disks, *Kyoto University Press*.

Kluźniak, W., Abramowicz, M. A. and Lee, W. H. (2004), High-frequency QPOs as a problem in physics: non-linear resonance, in P. Kaaret, F. K. Lamb and J. H. Swank, editors, *X-ray Timing 2003: Rossi and Beyond*, volume 714 of *American Institute of Physics Conference Series*, pp. 379–382, arXiv: `astro-ph/0402013`.

Kluźniak, W., Bulik, T. and Gondek-Rosińska, D. (2001), Quark stars in low-mass x-ray binaries: for and against, *Proceedings of the Fourth INTEGRAL Workshop, Ed: B. Battrick*, **ESASP 459**, p. 301.

Kluźniak, W., Lasota, J.-P., Abramowicz, M. A. and Warner, B. (2005), QPOs in cataclysmic variables and in X-ray binaries, *A&A*, **440**, pp. L25–L28.

Kluźniak, W. and Lee, W. H. (2002), The swallowing of a quark star by a black hole, *MNRAS*, **335**, p. L29.

Kluźniak, W. and Rosińska, D. (2013), Orbital and epicyclic frequencies of Maclaurin spheroids, *MNRAS*, **434**, p. 2825.

Mishra, B. and Vaidya, B. (2014), Geometrically thin accretion disk around Maclaurin spheroid, *A&A*, p. submitted.

Nowak, M. A. and Wagoner, R. V. (1991), Diskoseismology: Probing accretion disks. I - Trapped adiabatic oscillations, *ApJ*, **378**, p. 656.

Nowak, M. A. and Wagoner, R. V. (1992), Diskoseismology: Probing accretion disks. II - G-modes, gravitational radiation reaction, and viscosity, *ApJ*, **393**, p. 697.

Okazaki, A. T., Kato, S. and Fukue, J. (1987), Global trapped oscillations of relativistic accretion disks, *PASJ*, **39**, p. 457.

Paczyński, B. and Wiita, P. J. (1980), Thick accretion disks and superluminal luminosities, *A&A*, **88**, p. 23.

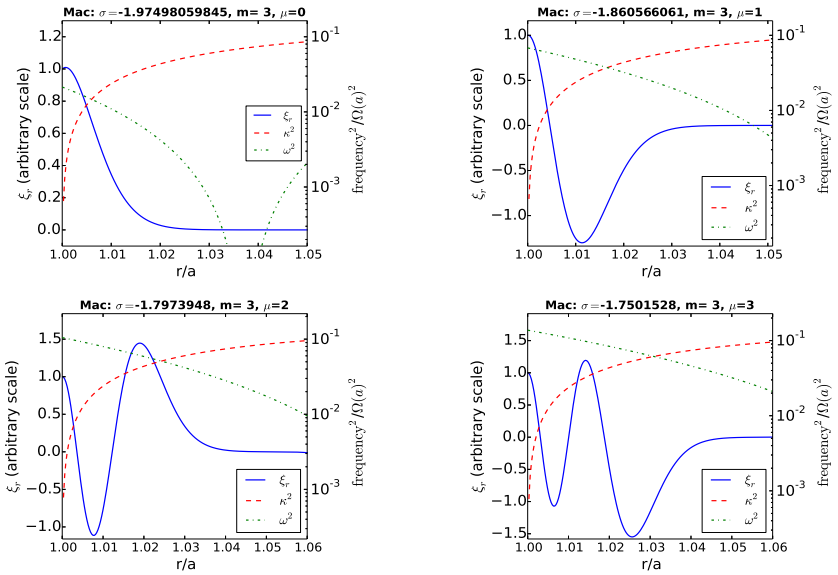

Figure 10. Same as Fig. 6, but for $m = 3$.

Perez, C., Silbergleit, A., Wagoner, R. and Lehr, D. (1997), Relativistic Diskoseismology. I. Analytical Results for "Gravity Modes", *ApJ*, **476**, p. 589.

Shakura, N. I. and Sunyaev, R. A. (1973), Black holes in binary systems. Observational appearance, *A&A*, **24**, p. 337.

Silbergleit, A., Wagoner, R. and Ortega-Rodríguez, M. (2001), Relativistic Diskoseismology. II. Analytical Results for C-modes, *ApJ*, **548**, p. 335.

Török, G., Abramowicz, M. A., Kluźniak, W. and Stuchlík, Z. (2005), The orbital resonance model for twin peak kHz quasi periodic oscillations in microquasars, *A&A*, **436**, pp. 1–8.

van der Klis M. (2000), Millisecond Oscillations in X-ray Binaries, *AnnRevA&A,*, **38**, p. 717.

Wagoner, R., Silbergleit, A. and Ortega-Rodríguez, M. (2001), "Stable" Quasi-periodic Oscillations and Black Hole Properties from Diskoseismology, *ApJ*, **559**, p. L25.

Woudt, P. A. and Warner, B. (2002), Dwarf nova oscillations and quasi-periodic oscillations in cataclysmic variables - I. Observations of VW Hyi, *MNRAS*, **333**, p. 411.

Zdunik, J. L. and Gourgoulhon, E. (2001), Small strange stars and marginally stable orbit in Newtonian theory, *Phys. Rev. D.*

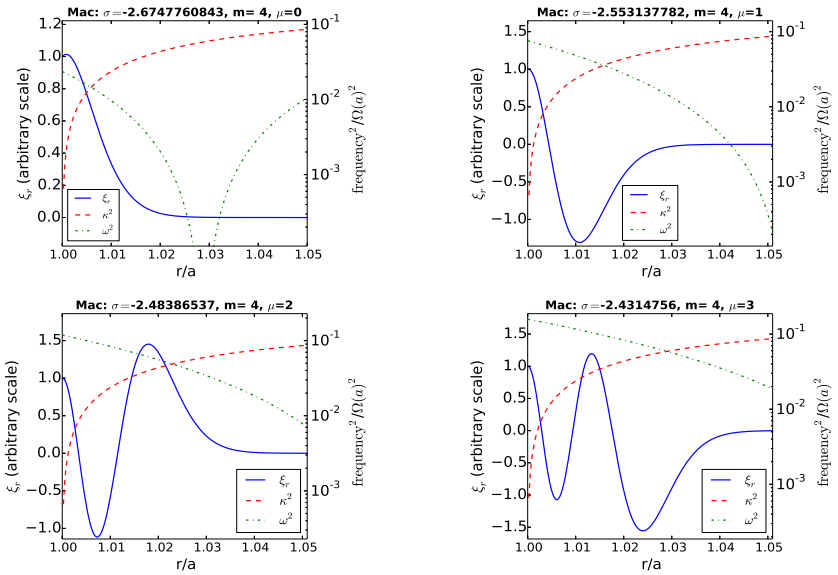

Figure 11. Same as Fig. 6, but for $m = 4$.